IEEE Access
Multidisciplinary | Rapid Review | Open Access Journal

Received February 24, 2020, accepted March 5, 2020, date of publication March 9, 2020, date of current version March 18, 2020.

Digital Object Identifier 10.1109/ACCESS.2020.2979476

On-Board Fast and Intelligent Perception of Ships With the "Jilin-1" Spectrum 01/02 Satellites

SHUHAI YU[1,2], YU YUANBO[1], XIAOJUN HE[1,3], MU LU[1], PENG WANG[1], XIANGDONG AN[1], AND XIUCHENG FANG[1]

[1]Chang Guang Satellite Technology Company Ltd., Changchun 130102, China
[2]Key Laboratory of Satellite Remote Sensing Application Technology of Jilin Province, Chang Guang Satellite Technology Company Ltd., Changchun 130102, China
[3]Changchun Institute of Optics, Fine Mechanics and Physics, Chinese Academy of Sciences, Changchun 130033, China

Corresponding authors: Shuhai Yu (yushuhai_0707@sina.com) and Xiaojun He (hexiaojun6@163.com)

This work was supported in part by the Pre-Research Project under Grant 31512020104-3, and in part by the Key Science and Technology Development in Jilin Province under Grant 20180201107GX.

ABSTRACT Acquisition of information on ocean-going vessels is important for trade, shipping safety and assessing illegal behavior, and so on. Optical remote sensing satellites have become important for the above tasks because of its advantages of a large swath width, high resolution and independence from ground basic resources. Relying on the "Jilin-1" Spectrum 01/02 satellites, this paper proposes an on-board processing system for ship information acquisition and is studied with the relevant methods. The main modules include data analysis, image preprocessing, target area recommendation, target detection, and longitude and latitude calculation of the ship. The paper utilizes a narrow-band communication channel to send a message to the user when the offshore ship's length is more than 70 m. The satellite-ground experiment shows that the information was acquired within 4 minutes from the intelligence system working to the operator getting the ship's information. The delay of information acquisition is reduced from a few hours in previous systems to a few minutes in this system. This paper the first attempt at intelligent on-board information processing in the field of commercial aerospace.

INDEX TERMS Optical remote satellite, on-board intelligent processing, ship information extraction, remote sensing image processing, "Jilin-1" Satellites.

I. INTRODUCTION

Ships are an important carrier of international commodities, so promoting transportation efficiency and safety, waterway planning, navigation monitoring, and emergency rescue, and so on, is useful work. Ship information acquisition should be the first step for the above jobs. Some multitype ground equipment are used extensively for inshore ship detection but are not suitable for ocean-going vessel supervision because of the geographical limitation. Satellites, which can obtain high-resolution data with large swath width and do not rely on on-the-ground basic resources, have become an important means for offshore ship supervision.

Synthetic aperture radar (SAR), with its all-weather imaging capability and low water reflection, has been widely used for ship detection. Researchers have attained many achievements on ship detection [1]–[3] with SAR imagery. SAR has the advantages of strong anti-interference and penetrating ability, but the data inversion processing is relatively complicated and does not meet human vision standards. Compared with SAR, optical remote sensing satellites have a large swath width and high resolution and can obtain detailed optical characteristics, which is why it has become one of the most important platforms for information assessment, such as for crop growth status monitoring, forest condition surveying, weather forecasting, environmental monitoring, city and water planning [4]–[6], and high-value target searching and tracking [7], [8].

The difference between SAR and optical remote sensing imagery makes it difficult to directly apply ship detection methods to optical remote sensing images. Thus, relevant scholars have performed many studies in related fields. For example, Yang *et al.* [9] adopted the saliency model and local binary pattern (LBP) features to achieve the extraction of ship

The associate editor coordinating the review of this manuscript and approving it for publication was Shaohua Wan.

This work is licensed under a Creative Commons Attribution 4.0 License. For more information, see https://creativecommons.org/licenses/by/4.0/

targets, with an accuracy reaching over 90%. Dong *et al.* [10] utilized the saliency and a rotation-invariant descriptor for ship detection, and used a support vector machine (SVM) classifier to detect real ships, and the accuracy reached 94%. He *et al.* [11] used a weighted voting method to detect inshore ships, and the detection accuracy reached more than 75%. Based on the characteristic of the "V" shape structure of the bow, Li [12] achieved port ship detection. Literature [13] summarized the vessel detection and classification by space borne optical images.

To improve the service capability, the swath width and resolution of the payload are increasingly improved, which augments the storage and data transmission requirements of the satellite platform. The traditional information acquisition method often results in a delay of several hours from satellite scanning because of the remote sensing application mode (command - satellite scanning - storage - data transmission - distribution - information extraction – user), as well as the geographic location limitation of the ground receiving system, which makes it difficult to meet the demand of rapid information acquisition of ships. In the field of ocean-going vessel detection, the proportion of vessel information and imaging data can be up to 0.001. Therefore, the traditional information acquisition method not only results in delays but is also a great waste of satellite resources. Transferring the traditional processing methods from the ground to the on-board processing system and merely transmitting the application service information is an effective approach to improve the timeliness.

According to the published literature at the present stage, multispectral information fusion is mostly adopted to extract ship information by inter-spectral features. However, in terms of the on-board application, spectral segmentation registration yields extravagant resource costs. Almost all of the ship identification processing methods are based on standard products with a high image quality, most of them only recognize local images, and the resolution is usually 640 pixels $\times$ 512 pixels. In addition, to improve the processing accuracy, the complexity of the algorithm is increased. On-board processing directly faces an original data stream on the order of GBs, which requires the system to complete the work under start-up time, power consumption and volume limitations. Therefore, relevant algorithm design should be carried out according to the actual requirements. Reference [14] combined constraints such as the length and width of the ship and realized the ship detection using a multispectral Sentinel-2 image and compared the results with the AIS information. Although high-quality standard images are still used in the literature, the algorithm complexity is more suitable for on-board application. Yuan Yao *et al.* used deep learning and a commercial off-the shelf (COTS) component to realize on-board ship detection using advanced product data [15]. Yu Ji-yang *et al.* adopted multiscale salience enhancement for ship detection [16]. The results were surprising but have yet to be verified in orbit.

After the ship information is extracted, another problem needs to be solved: how to transfer the information to the user quickly to meet the requirement of rapid information acquisition. However, there are few public reports for reference.

Based on the near-infrared spectrum (784.5 nm to 899.5 nm, with a ground resolution of 5 m per pixel @ 535 km) of the "Jilin-1" Spectrum 01/02 satellites, the sea-land and cloud segmentation methods are proposed, which improve the threshold adaptability. The paper used a pattern recognition approach to realize the recommended target area and detection, and combined with the auxiliary data information of satellite, the corresponding latitude and longitude of the target centroid are simultaneous recorded. The paper describes the processing system, data flow design, detection method, satellite-to-ground test, and so on. Their experiment shows that the user acquires the ship information within 4 minutes from processing.

The paper is organized as follows: the second chapter introduces the satellite platform and the on-board processing system; in the third chapter, the ship detection algorithm is described; in the fourth chapter, we describe the ground experiment and in-orbit test. The last chapter summarizes the research of this paper, discusses the advantages and disadvantages of the system, and describes future research work.

II. SATELLITE PLATFORM AND ON-BOARD PROCESSING SYSTEM

A. "JILIN-1" SPECTRUM 01/02 SATELLITES

The World Ocean occupies more than 71% of the earth's surface, so offshore ship searching requires optical remote sensing satellites to have a large swath width, which depends on the imaging electronics and optical design of the system. Constrained by the number of pixels of the imaging sensor, the imaging resolution and swath width are mutually restricted. For ship information acquisition, especially for ocean-going ships (ocean-going trade ships are generally longer than 100 m), it is feasible to select a medium resolution of 5-10 m.

Based on the progress made in technological research and the satellite launching node, the on-board processing system was carried on the "Jilin-1" Spectrum 01/02 satellites. The payload is a multispectral system with 20 spectra, so the resolution is lower than that of some optical or SAR satellites. Although the resolution of the optical payload is 5 m per pixel at 535 km, we can still verify the whole system, including the hardware and software of the processing system, for quick information distribution.

The Jilin-1 Spectrum 01/02 satellites are designed with an off-axis tri-reflection optical system, with a swath width of 110 km and a high-resolution imaging capability (5 m @ the star point). The payload has a full spectrum design (0.4 μm$\sim$13.5 μm), including visible, near-infrared, shortwave infrared, medium-wave and longwave infrared spectra. The optical payload consists of two spectrometers measuring 20 spectra, which weigh only 27 kg. The four

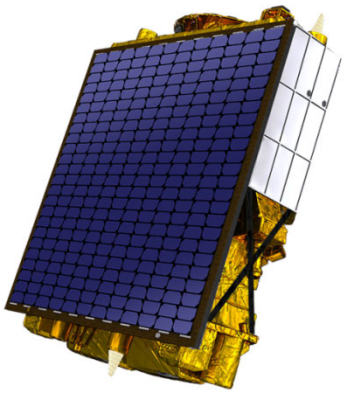

FIGURE 1. The 3D model of the satellite.

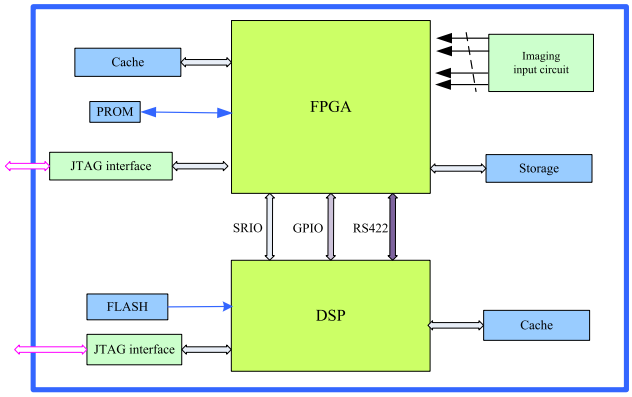

FIGURE 2. The structure of the processing system.

shortwave infrared spectra are segmented from 1190 nm to 1690 nm. The near-infrared spectrum has a resolution of 5 m per pixel, which is very effective for ship detection.

The 3D model of the satellite is shown in Fig. 1.

The satellite was launched at January 21, 2019 [17]. By October, a spectral image of China with a resolution of 5 m had been completed.

B. ON-BOARD PROCESSING SYSTEM

The on-board processing system adopts an FPGA+DSP hardware architecture to meet the requirements of multispectral big data storage, compression and identification. The calculation frequency of the processing system reaches over 10 GHz, and the software supports on-board updating for later functional upgrades. The structure of the processing system is shown in Fig. 2.

The FPGA is used as the controller for external interfaces and as the processor for the payload data storage, compression, information communication between the payloads and central computer, etc. A DSP is adopted as the ship detection processor. Although the deep learning method can realize an incredible detection accuracy, it requires some neural network calculations and works very well with the GPU processor. We adopted the pattern recognition method in this paper because of the use of a DSP as the processor.

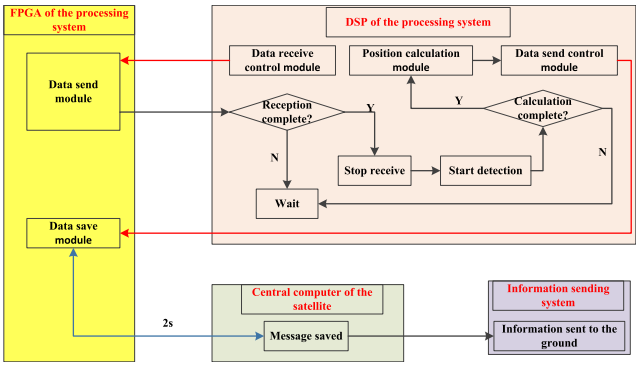

FIGURE 3. The data and message flow of the on-board processing system.

We have also performed some experiments on the "Jilin-1" gf03 satellites for ship and plane recognition using a GPU and a deep learning method.

The data and information flow of the on-board processing system is shown in Fig. 3. Data interaction between the FPGA and DSP is through the SRIO. GPIO and RS422 modules, which are used as a status controller, for instruction interaction and as a data communication channel, respectively. The FPGA sends a task start interrupt signal to the DSP by the GPIO module, and the DSP will send the interrupt signal to the FPGA when the import data volume is met during processing. The RS422 module sends task-type commands from the FPGA to the DSP, and the processing result will be reverse transmitted. The SRIO module is adopted to send remote sensing data from the FPGA to the DSP. When the received data meets the processing requirements, the DSP tells the FPGA to suspend data reception and runs the ship identification module. Combined with the auxiliary data of the satellite, the longitude and latitude will be calculated for the centroid of the detected object then will be sent to the storage module of the FPGA. The FPGA and central computer of the satellite communicate every 2 s during the process, and the result is recorded by the satellite and transmitted to the ground terminal by a narrow-band communication channel.

The weight and the volume are 4.5 kg and 280 mm × 297 mm × 180 mm, respectively. The power consumption is approximately 75 W, including that of the other system, which is approximately 28 W. It is important to note that the on-board processing system needs to store the data of multitype payloads to process compression and transmission at the same time. Therefore, the weight and volume are required by the satellite and are not constrained by the on-board processing system. If only the intelligent perception function is implemented, the power consumption is approximately 18 W.

A picture of the processing system is shown in Fig. 4.

III. THE SHIP DETECTION ALGORITHM

Most of the time, a ship is either docking or sailing in the water, and the effect of background segmentation determines the accuracy of target recognition. Because of the high absorption rate and low reflectivity of water bodies at

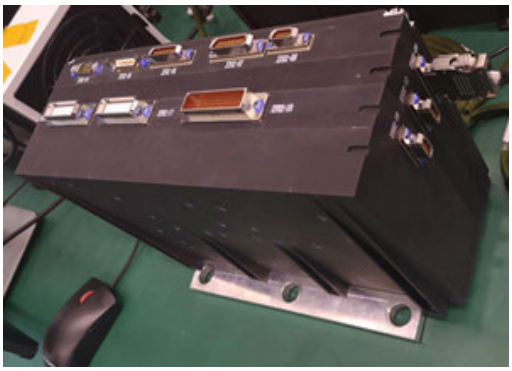

FIGURE 4. The image of the on-board processing system.

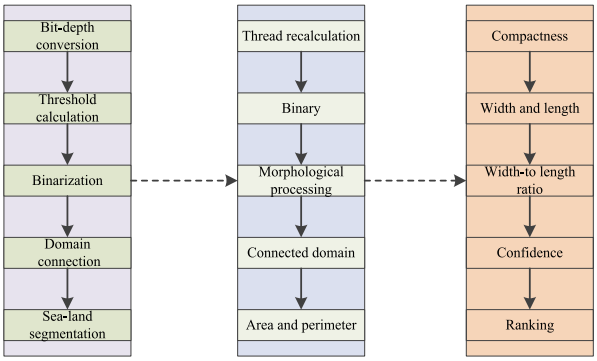

FIGURE 5. The flow chart of the ship identification algorithm.

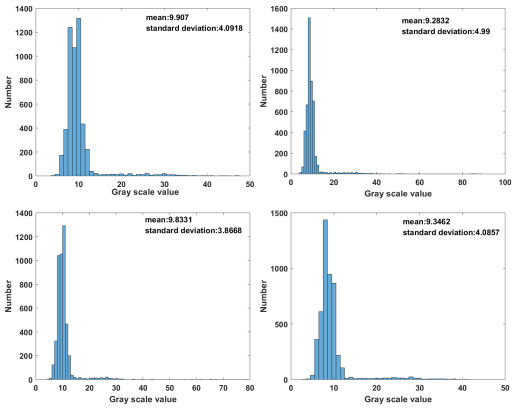

FIGURE 6. The histogram, mean and variance in the ship in the near-infrared band of "Jilin-1" Spectrum 01 satellite.

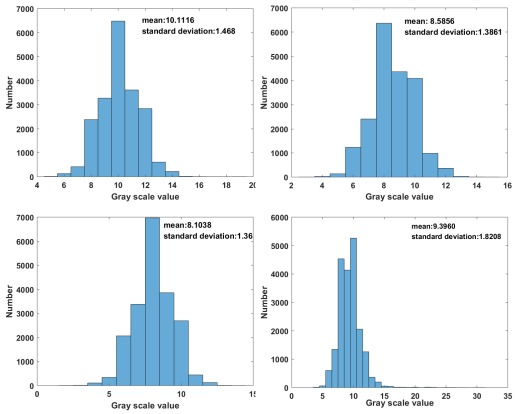

FIGURE 7. The histogram, mean and variance in the sea surface in the near-infrared band of the "Jilin-1" Spectrum 01 satellite.

the near-infrared spectrum, the paper adopts the B6 segment image of the Spectrum 01/02 satellites as the image data for processing.

The overall design of the algorithm, which is divided into three parts, is shown in Fig. 5. The first part is an image preprocessing step, which includes image bit-depth conversion and sea-land segmentation. The second part is the object recommendation step, including the threshold recalculation, analysis of the target's area and perimeter, and the calculation of their ratio. Finally, the third part extracts further information on object, adopts the compactness to realize accurate identification of the ship target, and ranks the confidences.

A. PREPROCESSING

To improve the information acquisition ability of the optical remote sensing satellite, the quantization of the image sensor is generally 12-16 bits. In on-board processing, the small bit depth contributes little in object recognition; moreover, to reduce the resource costs of the processing hardware, the paper first transforms the remote sensing image to an 8-bit image. The conversion formula is as follows:

$$img8bit = 255 \times [(img - \min(img))/\max(img) - \min(img)] \quad (1)$$

where img represents the near-infrared spectrum image acquired by the remote sensing satellite and $img8bit$ is the converted image; $\max(\cdot)$ and $\min(\cdot)$ are the maximum and minimum values of the image data, respectively.

The goal of the object detection algorithm is to find the difference between the target and the background, and image binarization is an important approach for foreground and background segmentation in the field of pattern recognition. The reflectivity of water (except in the direction of the specular reflection) is lower for all wavebands, generally approximately 3%, and more prominent in the near-infrared spectrum. Clean water almost becomes a full absorber after 750 nm, such as in the near-infrared band [18]. Reference [19] also discussed the advantage of using the near-infrared band for separating the water-column. We analyze the histogram, mean and variance of the ship and background area, as shown in Fig. 6 and Fig. 7. Although they are all have concentrated gray distributions, the variance in the ship area is obviously larger than that in the background, as shown in Fig. 6; the variance is 3-5 and 1.2-1.8 in Fig. 6 and Fig. 7, respectively. Therefore, we can use the difference in the variance to segment the object. The specific threshold calculation and segmentation methods will be described in the following.

To improve the on-board robustness of the processing system, two kinds of thresholding schemes are proposed: adaptive thresholding in orbit and up-linking instruction. For the adaptive threshold, the iterative optimal thresholding method is adopted. Affected by the high reflectivity of islands and clouds, the calculated threshold is relatively high. If this threshold is adopted, the ship will be filtered out as background, so it is difficult to realize ship detection. Therefore, this paper proposes a sea-land or cloud segmentation method. The adaptive threshold of the 8-bit image is calculated and multiplied by a coefficient as the first segmentation threshold, with the coefficient of 0.8 in this paper.

➢ Threshold calculation

Step 1: Set the initialization threshold T_{i} of the 8-bit image to 127.

Step 2: Calculate the modified value

Construct two sets by the following formula:

$$\begin{aligned} B\{k\} &= img8bit(i,j) \geq T_i \\ \mathrm{S}\{\mathrm{m}\} &= img8bit(i,j) < T_i \end{aligned} \tag{2}$$

Calculating the sum of the above formulas as follows:

$$\begin{aligned} DN_1 &= \sum_{k=1}^{K} B\{\mathrm{k}\} \\ DN_2 &= \sum_{m=1}^{M} \mathrm{S}\{\mathrm{m}\} \end{aligned} \tag{3}$$

where K and M are the number of set elements.

The calculation formula of the modified initialization threshold is as follows:

$$T_{\mathrm{r}} = (DN_1/K + DN_2/M)/2 \tag{4}$$

Step 3: Iterate

The paper denotes the iteration time as I_{t} and initially sets it to zero. The iterative method is as follows:

while $(T_{\mathrm{r}} - T_{\mathrm{i}}) > 2 \&\& (I_{\mathrm{t}} < 50))$

{

$I_{\mathrm{t}}++;$

$T_{\mathrm{i}} = T_{\mathrm{r}};$

Execute Step 2;

Save T_{r};

}

After the iterative calculation, we obtain the adaptive threshold for binarization, denoted by T. Then, the binary image can be obtained as follows:

$$BI(x,y) = \begin{cases} 255 & (DN(x,y) \geq 0.8 \times T) \\ 0 & (DN(x,y) < 0.8 \times T) \end{cases} \tag{5}$$

where $DN(x, y)$ represents gray value of image. (x, y) are the coordinates of a pixel at x and y.

Then, 8-connected domain detection processing is adopted for the binary image and generates the list. The paper assumes that the area and perimeter of the connected domain greater than the set threshold are interference objects, such as clouds, reefs and even land. The filtered connected domain binary image can be obtained by the following formula.

$$C(k) = \begin{cases} 0 & (S_C(k) \geq S_{CT} || P_C(k) \geq P_{CT}) \\ 255 & else \end{cases} \tag{6}$$

where $S_C(k)$ and $P_C(k)$ represent the area and perimeter, respectively, of the k-th connected domain. S_{CT} and P_{CT} are the thresholds of the area and perimeter of the connected domain, respectively.

The length and width of a ship is generally less than 350 m and 70 m, respectively. Therefore, in this paper, S_{CT} and P_{CT} are set to 8750 pixels and 285 pixels, respectively, because the resolution of the "Jilin-1" Spectrum 01/02 satellites is 5 m per pixel.

B. REGIONAL RECOMMENDED

The mask image can be obtained through the image C and $img8bit$ as shown as the following formula.

$$img_2 = img8bit \times C \tag{7}$$

After the above image processing step, the large areas of clouds, land, islands, reefs and other high-reflectivity features are removed, and the gray value of the mask image is very small. The remaining image includes the large area of the sea surface and some potential ships, so the uniformity is very good. Compared with the swath width of optical satellite, the pixels of background are much greater than that of the objects, so we adopted the second-order threshold method to calculate the new threshold, which is widely used in the star sensor domain.

$$T_2 = M + \mathrm{a} \times \delta \tag{8}$$

where M and δ are the mean and variance for the resulting image; a is a coefficient and is set to 2.

To reduce the influence of outliers and waves on target extraction, morphological processing, including corrosion and expansion. is carried out. First, the expansion and corrosion operations are adopted sequentially with a 3×3 rectangle as the kernel function. Then, to keep the empty areas in the target from impacting the subsequent calculation of the target scale, the expansion processing operation is used for the corrosion image with the 3×3 rectangle kernel and is iterated two times. Finally, the corrosion operation is adopted. After the image has been morphologically processed, the outer connected domain is calculated again.

If the ratio of the area to the perimeter and the compactness both satisfy the following formula, the k-th connected domain is considered the recommended region, otherwise it is regarded as invalid.

$$\begin{cases} S_C(k)/P_C(k) > 2.5 \\ \pi \times S_C(k)/P_C(k)^2 > 0.05 \end{cases} \tag{9}$$

The paper expands the target area by 20 pixels as the ROI and enters the next level to perform more complex calculations for refined detection.

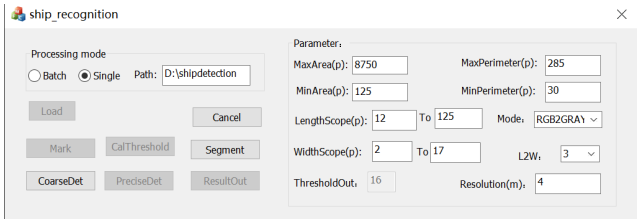

FIGURE 8. The software platform.

C. SHIP DETECTION

The reference "A Direct and Fast Methodology for Ship Recognition in Sentinel-2 Multispectral Imagery" proposed the calculation methods of the target length, width and rotation angle in the connected domain. The specific processing steps can be seen in the supplementary materials of the paper. The threshold value of the target length and width is 50 m-500 m and 10-70 m, respectively, in this paper. The threshold of the length-to-width ratio of the object is set to 3. The degree of confidence is calculated for the target that satisfies the aspect ratio, as in the following formula:

$$Con = C_{sum}/L/W \tag{10}$$

where C_{sum} is the number of nonzero pixels in the connection and L and W are the length and width of object, respectively.

Due to the noninteger problem during calculation and to avoid the degree of confidence being greater than one after processing, a judging method is adopted, and the confidence values are ranked from largest to smallest for storing and transmitting the target information with high confidence.

IV. EXPERIMENTS

A. EXPERIMENT

The software platform is designed as shown in Fig. 8. The images of the "Jilin-1" video satellites, which captured by the push-sweep working mode, are used as the data source for algorithm verification. The resolution of the near-infrared image is 3.68 m per pixel, which is rounded to 4 m in this paper. The platform includes the import parameter, the threshold display and an image storage module.

To reduce the computational cost, we optimize the scheduling of the internal calculation modules. The most complex part is the connected domain, so to avoid duplicate calculations, the step of second connected domain is only executed for the recommended region.

The result of different processing stage is shown in Fig. 9. Fig. 9 (a) is the 16-bit original image; Fig. 9 (b) is obtained by binarization with the threshold value calculated by formula 5; Fig. 9 (c) is sea-land segmentation using formula 6, which can restrain the large areas to influent subsequent processing, such as land, cloud, and reefs; Fig. 9 (d) is the mask image derived through formula 7. It is important to note that the mask image is 8-bits per pixel. Because we have subtracted the large areas, the image looks similar to the black image. Fig. 9 (e) is regional recommendation image; the region recommendation is indicated by the rectangular box, including eight ships and four false-alarm areas; Fig. 9 (f) shows the detection results, and only eight ships are identified.

TABLE 1. The information on the ships.

No.	Conf	x	y	Wi	Hi	Wo	Lo
1	0.9998	747	1468	47	51	7.47	37.05
2	0.9963	765	2071	39	57	8.58	38.16
3	0.9911	727	1295	51	53	8.90	40.31
4	0.9844	897	1333	45	54	8.50	37.75
5	0.9838	859	1945	39	46	7.344	28.54
6	0.9822	653	1875	42	56	9.01	37.92
7	0.9801	944	1675	44	56	8.77	38.00
8	0.9765	750	1692	41	57	8.84	37.99

The original image is stored as a 16-bit image, so it is a black figure. After applying the adaptive threshold, the binarized image can display the reflected land. It can be seen from the figures that the proposed algorithm can extract ships well under land and reef interference. The binary ROI image after the region recommendation is shown in Fig. 10. The binary and 8-bit images of the ROIs after the final detection are shown in Fig. 11 and Fig. 12, respectively.

As seen from Fig. 12, when the difference between the ships and background is very small, the system can still achieve accurate ship detection.

The information on the ships is shown in Tab. 1.

In this table, Conf is the confidence, x and y are the pixel coordinates of the ROI in the upper-left corner of the target region. Wi and Hi are the width and height of the target area, respectively. Wo and Lo represent the width and length of the ship, respectively. The units of Wi, Hi, Wo and Lo are pixels.

We also compare the important parameters as shown in Fig. 13, such as the factor of first binarization as shown in formula 5, the method for solving the second coefficient threshold solving in formula 8, and the area, perimeter and compactness.

To evaluate the object detection performance, we calculate the precision, recall and accuracy.

The precision reflects the false detection rate, and the formula is as follows:

$$Precision = \frac{N_{tp}}{N_{tp} + N_{fp}} \tag{11}$$

where the N_{tp} is the number of correctly detected objects and the N_{fp} is the number of falsely detected objects.

The recall represents the effectiveness of the detection and is defined by the following formula.

$$Recall = \frac{N_{tp}}{N_{tp} + N_{fn}} \tag{12}$$

where N_{fn} is the number of undetected ships.

The accuracy expresses the correctness for all the samples.

$$Accuracy = \frac{N_{tp} + N_{tn}}{N_{ap} + N_{an}} \tag{13}$$

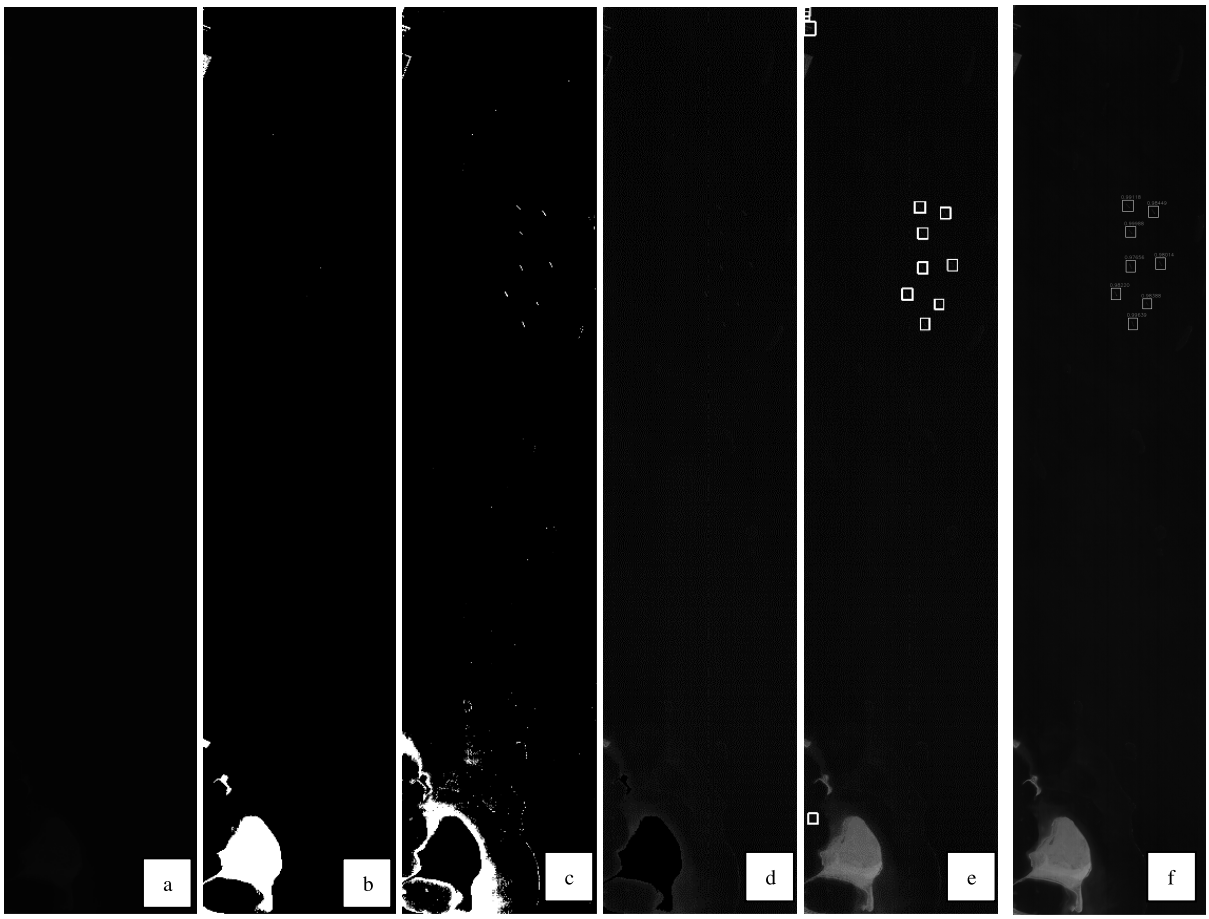

FIGURE 9. The result of main processing step. (a) original image, (b) binarized image, (c) sea-land segmentation, (d) mask image, (e) region recommendation, and (f) final detection results.

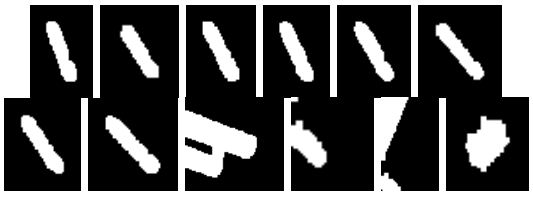

FIGURE 10. The binary images of the ROIs after regional recommendation.

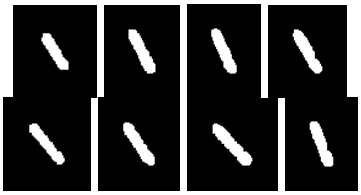

FIGURE 11. The binary images of the ROIs after the final detection.

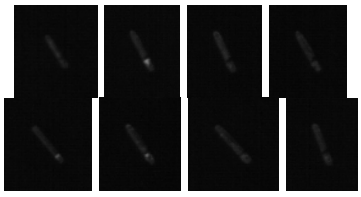

FIGURE 12. The 8-bit image of the ROIs after the final detection.

TABLE 2. The number of samples and detected counts.

N_{ap}	N_{an}	N_{tp}	N_{fp}	N_{fn}	N_{tn}
298	191	248	16	50	175

TABLE 3. The evaluation of the detected performance.

Method	Precision (%)	Recall (%)	Accuracy (%)
CFAR	87.2	85.82	81.72
Our	93.93	83.22	86.50

where N_{tn} is the number of detected negative samples, the N_{ap} and N_{an} is the number of positive and the negative samples, respectively.

We compare our method adopted in paper with the Constant False-Alarm Rate (CFAR). The evaluation of detected performance is shown in Tab.3. It is note to that the CFAR is sensitive to the land or clouds, hence, we use the sea-land segmentation image for CFAR processing.

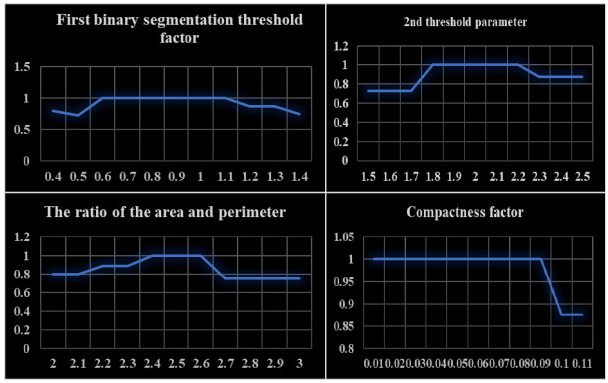

FIGURE 13. Statistics on the influence of important parameters on the results.

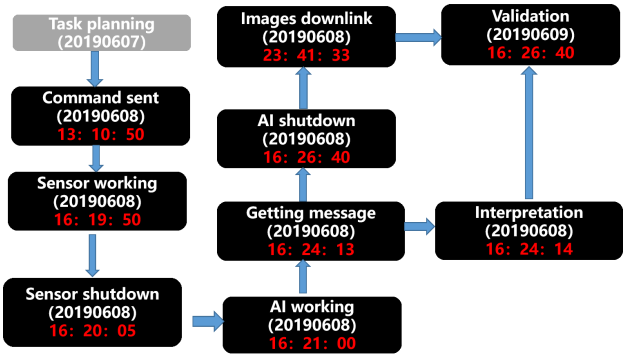

FIGURE 14. Task flow of satellite and ground synchronization validation.

FIGURE 15. The processing image and the ROI.

B. ON-BOARD TEST

The Spectrum 01/02 satellites were launched into orbit on January 21, 2019, and since April 16, 2019, the ship autonomous search test was conducted.

We adopt 12,000 pixels × 1,000 pixels as the processing unit and handle each unit one by one. We choose the ship search test on June 7, 2019, as the example to describe the test flow and results, as shown in Fig. 14. The imaging time (Beijing time) was 16:19:54, the on-orbit processing system was switched on at 16:21:00, and the results were sent to the ground at 16:24:14. The remote sensing image was received at 23:41:33, and the image data processing and production were completed at 16:26:40 on June 9. By comparison, it can be found that the delay in obtaining the ship information is within just 4 minutes.

The ship information includes the position (25.517754°N, 54.724251°E) and the scale (width of approximately 45 m, length of approximately 270 m). The processing image is shown in Fig. 15.

The received message and decodings are shown in Tab. 4.

The other test results are shown in Tab. 5.

TABLE 4. The received messages and decodings.

No.	Code	Meaning	Frame number	Source code	Decoding
1	ZT-C001	Frame synchronization code	3	0xEB90	60304
2	ZT-C002	Satellite identification code	3	0x41	GP01
3	FB-C000_2	Time in seconds	3	0x248D8368	2019/6/8 16:19
4	FB-C000_3	Decimal seconds	3	0x0A1D00	662784
5	FB-C001_2	E or W mask	3	0x00	E
6	FB-C002_2	Target longitude	3	0X26D6A2	54.724251
		position			
7	FB-C003_2	S or N mask	3	0x00	S
8	FB-C004_2	Target latitude position	3	0x240D83	25.517754
9	FB-C005_2	Height	3	0x36	270
10	FB-C006_2	Width	3	0x09	45

TABLE 5. The other test results.

Number	Category	Test date	Results
1	Ship	4.16	Four ships
2	Ship	6.7	None
3	Ship	6.8	One ship
4	Ship	6.9	None
5	Ship	6.10	None
6	Fire	3.21	Two fire points
7	Cloud	2.1	Thick clouds were detected

V. CONCLUSION

To improve the capability of remote sensing satellites in ship searching and information acquisition tasks, based on the "Jilin-1" Spectrum 01/02 satellites, this paper realizes the whole process of on-board ship detection, information extraction and rapid distribution. Aiming at the influence of ground objects on ship detection, a method of sea-land and cloud segmentation are proposed to realize high-precision detection under the condition that the

difference between ships and background gray values is small. The laboratory experiment and in-orbit test verification were carried out, and the delay in information acquisition was reduced from the previous few hours to a few minutes, which was the first attempt at intelligent on-board information processing in the field of commercial aerospace.

We will continue to research processing algorithms and platform optimization to further improve the information processing capacity and efficiency.

REFERENCES

[1] C. Wang, S. Jiang, H. Zhang, F. Wu, and B. Zhang, "Ship detection for high-resolution SAR images based on feature analysis," *IEEE Geosci. Remote Sens. Lett.*, vol. 11, no. 1, pp. 119–123, Jan. 2014.

[2] W. An, C. Xie, and X. Yuan, "An improved iterative censoring scheme for CFAR ship detection with SAR imagery," *IEEE Trans. Geosci. Remote Sens.*, vol. 52, no. 8, pp. 4585–4595, Aug. 2014.

[3] B. Hou, X. Chen, and L. Jiao, "Multilayer CFAR detection of ship targets in very high resolution SAR images," *IEEE Geosci. Remote Sens. Lett.*, vol. 12, no. 4, pp. 811–815, Apr. 2015.

[4] M. Immitzer, F. Vuolo, and C. Atzberger, "First experience with Sentinel-2 data for crop and tree species classifications in central Europe," *Remote Sens.*, vol. 8, no. 3, p. 166, 2016.

[5] Z. Chen, J. Ren, H. Tang, Y. Shi, and J. Liu, "Progress and perspectives on agricultural remote sensing research and applications in China," *J. Remote Sens.*, vol. 20, no. 5, pp. 748–767, 2016.

[6] H. Li, Z.-X. Chen, Z.-W. Jiang, W.-B. Wu, J.-Q. Ren, B. Liu, and H. Tuya, "Comparative analysis of GF-1, HJ-1, and Landsat-8 data for estimating the leaf area index of winter wheat," *J. Integrative Agricult.*, vol. 16, no. 2, pp. 266–285, Feb. 2017.

[7] C. Corbane, L. Najman, E. Pecoul, L. Demagistri, and M. Petit, "A complete processing chain for ship detection using optical satellite imagery," *Int. J. Remote Sens.*, vol. 31, no. 22, pp. 5837–5854, Dec. 2010.

[8] H. Heiselberg, "A direct and fast methodology for ship recognition in Sentinel-2 multispectral imagery," *Remote Sens.*, vol. 8, no. 12, p. 1033, 2016.

[9] F. Yang, Q. Xu, and B. Li, "Ship detection from optical satellite images based on saliency segmentation and structure-LBP feature," *IEEE Geosci. Remote Sens. Lett.*, vol. 14, no. 5, pp. 602–606, May 2017.

[10] C. Dong, J. Liu, and F. Xu, "Ship detection in optical remote sensing images based on saliency and a rotation-invariant descriptor," *Remote Sens.*, vol. 10, no. 3, p. 400, 2018.

[11] H. He, Y. Lin, F. Chen, H.-M. Tai, and Z. Yin, "Inshore ship detection in remote sensing images via weighted pose voting," *IEEE Trans. Geosci. Remote Sens.*, vol. 55, no. 6, pp. 3091–3107, Jun. 2017.

[12] S. Li, Z. Zhou, B. Wang, and F. Wu, "A novel inshore ship detection via ship head classification and body boundary determination," *IEEE Geosci. Remote Sens. Lett.*, vol. 13, no. 12, pp. 1920–1924, Dec. 2016.

[13] U. Kanjir, H. Greidanus, and K. Oštir, "Vessel detection and classification from spaceborne optical images: A literature survey," *Remote Sens. Environ.*, vol. 207, pp. 1–26, Mar. 2018.

[14] Y. Yao, Z. Jiang, H. Zhang, and Y. Zhou, "On-board ship detection in micro-nano satellite based on deep learning and COTS component," *Remote Sens.*, vol. 11, no. 7, p. 762, 2019.

[15] Y. Ji-yang, H. Dan, W. Lu-yuan, L. Xin, and L. Wen-juan, "On-board ship targets detection method based on multi-scale salience enhancement for remote sensing image," in *Proc. IEEE 13th Int. Conf. Signal Process. (ICSP)*, Nov. 2016, pp. 217–221.

[16] S. Haowei, "LM-11 starts China's commercial launch activity in 2019," *Aerosp. China*, vol. 20, no. 1, p. 61, 2019.

[17] L. Richard Miller, E. Carlos Del Castillo, and A. Brent McKee, *Remote Sensing of Coastal Aquatic Environments*. Amsterdam, The Netherlands: Springer, 2005, pp. 83–146.

[18] E. J. D'Sa, C. Hu, F. E. Muller-Karger, and K. L. Carder, "Estimation of colored dissolved organic matter and salinity fields in case 2 waters using SeaWiFS: Examples from florida bay and florida shelf," *J. Earth Syst. Sci.*, vol. 111, no. 3, pp. 197–207, Sep. 2002.

SHUHAI YU was born in China, in 1985. He received the B.S. degree from Jilin University, in 2009, and the Ph.D. degree from the Changchun Institute of Optics and Mechanics, Chinese Academy of Sciences, in 2014.

He worked as an Assistant Researcher with the Changchun Institute of Optics and Mechanics from 2014 to 2016. In April 2016, he joined Chang Guang Satellite Technology Company Ltd. He has published more than ten research articles and two authorized invention patents. As a member of the two satellite models of the general group, completed the two models of the satellite development work. As a host and a major member, he has participated in more than ten projects. His research interests include on-board intelligent processing of satellites, image processing, and optical imaging technology.

YU YUANBO was born in 1993. He received the bachelor's degree from the University of Science and Technology of China, and the master's degree in mechanical engineering from the Changchun Institute of Optics, Fine Mechanics and Physics, Chinese Academy of Sciences (CAS). He is mainly engaged in the satellite's on-orbit information processing systems.

He has been in charge of Jilin NO.1 spectral 01/02 on-orbit information processing systems.

XIAOJUN HE was born in Guang'an, Sichuan, China, in 1983. He received the B.S. degree from Jilin University, in 2016, and the Ph.D. degree from the Chinese Academy of Sciences, in 2011.

He is currently the Director of the photoelectric imaging room with Chang Guang Satellite Technology Company Ltd., and the Chief of the Spectrum Series Satellite. He is also responsible for the overall development of the load electronics system and the spectrum series satellites and has long been committed to the research of new imaging technologies. His relevant research results are widely used in the Jilin-1 Satellite. As a major member, he has participated in more than ten aerospace projects such as 863, natural fund, and final assembly research. He has published more than ten articles and granted two patents.

Dr. Xiaojun was a member of the national "Nuclear High Base" 01 special expert group. He was selected as the first batch of the Research and Development Talent Team of major science and technology projects in Jilin Province. He received the First Prize of the Army Science and Technology Progress Award (ranked ninth).

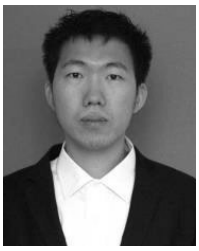

MU LU was born in Changchun, China, in 1989. He received the B.E. and M.E. degrees in communication engineering from Jilin University, in 2012, and the Ph.D. degree in mechatronic engineering from the University of Chinese Academy of Sciences, in 2017.

His research interests include digital imaging processing and moving target detection and multitarget tracking and moving target recognition.

PENG WANG was born in 1988. He received the bachelor's degree, in 2010, and the master's degree from Jilin University, in 2013.

He currently works with the Optoelectronic Imaging Department, Chang Guang Satellite Technology Company Ltd. He is also an ordinary FPGA Logic Engineer and has been employed by Foxconn and H3C Group Technology Company Ltd. to engage in the research and development of server and network products.

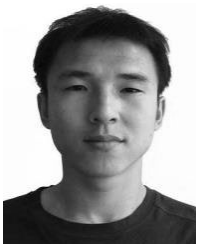

XIANGDONG AN was born in 1991. He received the bachelor's and master's degrees from the National Laboratory of Antenna and Microwave Technology, Xidian University, Xi'an, Shaanxi, China.

He is currently a Junior Research Intern with Chang Guang Satellite Technology Company Ltd. His research interests include satellite AIS payload and satellite antenna.

XIUCHENG FANG was born in 1990. He received the master's degree from the College of Instrumentation and Electrical Engineering, Jilin University.

He is currently working on Telemetry Software of Jilin-1 Satellite's Constellation and engaging in satellite telemetry data parsing and satellite status monitoring.